The 3D Visibility Complex: a unified data-structure for global visibility of scenes of polygons and smooth objects

Frédo Durand, George Drettakis, Claude Puech

The 3D Visibility Complex: a unified data-structure for global visibility of scenes of polygons and smooth objects

Frédo Durand, George Drettakis and Claude Puech
*i*MAGIS-GRAVIR/INRIA *

Abstract

In this paper we describe a unified data-structure, the *3D Visibility Complex* which encodes the visibility information of a 3D scene of polygons and smooth convex objects. This data-structure is a partition of the maximal free segments and is based on the characterization of the topological changes of visibility along critical line sets. We show that the size k of the complex is $\Omega(n)$ and $O(n^4)$ and we give an output sensitive algorithm to build it in time $O((n^3 + k)\log n)$.

This theoretical work has already been used to define a practical data-structure, the *Visibility Skeleton* described in a companion paper.

1 Introduction

Visibility is a crucial issue; motion planning in robotics, object recognition in computer vision, lighting simulation or view maintenance in computer graphics are some examples where global visibility computations are required. The notion of "coherence" is often cited as the key to treat these problems efficiently and not restart every computation from scratch, but its characterization is not straightforward.

The usual space-subdivision methods do not translate the line nature of visibility, since a line of sight intersects many cells of any subdivision.

Computational geometers have characterized sets of lines in space by using Plücker duality. It is an oriented projective 5D dual space in which lines of space are naturally and linearly embedded (lines intersecting a given line are associated with hyperplanes). Its main drawback is the necessity of an intersection with the Plücker hypersurface [CEG+96, Pel90]. The scenes considered have always been polygonal and are mainly restricted to isothetic or c-oriented polygons. (In fact there exists a few results on ray-shooting with spheres involving parametric search without Plücker coordinates [MS97]). These techniques have been used by Teller in computer graphics to compute the antipenumbra cast by an area light source through polygonal portals [Tel92]. The problem with these methods is that intersections of lines with the entire scene are considered; occlusion is not really treated.

In computer vision, the *aspect graph* has been developed to characterize the viewpoints from which the scene has the same topological aspect. The viewing space (S^2 for orthographic projection, R^3 for perspective projection) is partitioned along *visual events*. Construction algorithms have been developed for polygons and algebraic objects, both for orthographic and perspective projection, and some of them have been implemented; see [EBD92] for a good survey. A main drawback of aspect graphs is their size: $O(n^6)$ for orthographic projection, and $O(n^9)$ for perspective projection.

To build the aspect graph, Plantinga and Dyer [PD90] defined an intermediate data structure called the *asp*. For the orthographic case, it is a partition of the 4D space of oriented lines of space according to the first object they hit, and for the perspective case it is a partition of the 5D space of oriented half lines (rays). This approach has been limited to polygonal scenes. It was applied to maintain views, but the degrees of freedom allowed by the implementation were limited to rotation along a predefined axis [PDS90].

In lighting simulation, researchers have computed the discontinuities of the lighting function (which correspond to the limits of umbra and penumbra) also called *discontinuity meshes*. This characterizes the visibility of a light source. Initially only a subset of discontinuities where computed (e.g., [LTG93]), followed by algorithms computing all the discontinuities, together with a structure, the *backprojection*, which encodes the topological aspect of the light source[DF94, SG94]. These approaches are nonetheless restricted to a single light-source at a time.

Recently, a data-structure which encodes all the visibility information of a 2D scene called the *Visibility Complex* has been defined [PV96]. This structure is a partition of the set of maximal free segments according to the object they touch. Optimal construction algorithms have been developed for smooth convex objects [PV96] as well as polygons [Riv97] and used for lighting simulation [ORDP96].

In [DDP96] we introduced the *3D Visibility Complex* for

scenes of convex smooth objects (the polygonal case was simply mentioned). An $O(n^4 \log n)$ brute-force algorithm was roughly sketched, and applications for lighting simulation, walkthroughs and aspect graph computation were proposed.

In this paper, we present a unified version of the 3D visibility complex for scenes of polygons and smooth convex objects. It is based on a complete catalogue of critical line sets which are lines where visibility changes. We derive bounds for the size of the complex and present an output sensitive construction algorithm.

Moreover, the formalism described in this article has been used to develop and implement a global visibility datastructure called the *Visibility Skeleton* [DDP97]. It is a simplified version of the 3D visibility complex for polygonal scenes built using a brute-force algorithm.

2 Scenes and maximal free segments

We consider scenes of polygons and algebraic smooth convex objects. Concave objects and piecewise smooth objects are beyond the scope of this article but could be handled by considering other critical line sets described by the theory of singularity [PPK92, Rie87]. The algebraic objects are assumed to have bounded degree. In what follows, n represents the overall complexity of the scene which is the total number of objects, polygons, edges and vertices. The objects are assumed to be in general position; degeneracy issues are not addressed in this paper.

In this work we do not consider lines but maximal free segments to take occlusion efficiently into account. Intuitively, a segment represents a class of rays, and we want to group the rays that "see" the same objects. Since many segments can be collinear, we need a fifth dimension to distinguish them. But it is not a continuous dimension: there is only a finite number of segments collinear to one line. See figure 1(a) where a 2d equivalent is shown. The segments a and b are collinear, t is tangent to the object and is adjacent to segments above and below the object. Topologically we have a branching structure represented in fig. 1 for parallel segments. Note that almost everywhere the graph is locally 1-dimensional. Similarly in 3D, the segment space is a 4D space embedded in 5D. This can be seen as a unification of the spaces used by Plantinga and Dyer [PD90]: in the orthographic case they deal with a 4D space and in the perspective case with a 5D space.

We use the same parameterization for lines as [PD90, DDP96]: they are represented by two coordinates of direction, the angles θ (azimuth) and φ (elevation) which are the spherical coordinates of the director vector, and the coordinates (u, v) of the projection onto the plane perpendicular to the line and going through the origin (the axes of of the plane are chosen such as u is orthogonal to both the director vector and the vertical). See figure 1(b). Note that if φ is fixed we obtain all the lines contained in a set of parallel planes.
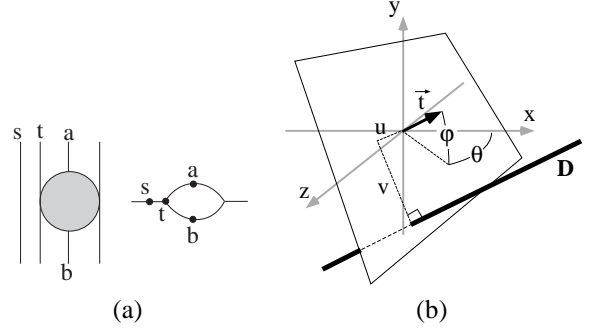

Figure 1: (a) 2D equivalent of the segment space: Parallel segments in the scene and local topology with branchings. (b) Parameterization of lines in space.

We call it a φ-slice. If we also fix v, we obtain the lines of a plane in which θ and u are the polar coordinates. We call it a φv-slice.

3 Critical segments

We define a segment to be in general position if it touches objects only at its extremities. A segment that touches objects in its interior will be called *critical*. At such an intersection there is a *local event*. If a segment touches more than one object in its interior, we call this a *multilocal event*. Critical segments are grouped into *critical segment sets*. The dimension of such a set can be seen as the number of degrees of freedom a segment has to keep the events. We can also refer to the codimension of such a set, which is the complement to the dimension of the space (the number of fixed degrees of freedom).

For the class of scenes we consider, there are two kinds of local events: tangency events and vertex events. The object or the vertex are called the *generators* of the event. To stay tangent to an object, a segment has three degrees of freedom. It is of codimension 1. It is of course the same when a segment goes through the edge of a polygon. We call this a T event from tangency (also referred to as E from edge in the aspect graph or discontinuity meshing literature which deals with polygonal scenes). A segment that goes through a vertex has two degrees of freedom (rotation), and thus has codimension 2. We call it a V event.

The combination of many local events causes a multilocal event, and the codimensions are added. We use the notation $+$ to describe such a combination. For example, a segment that is tangent to an object and that goes through a vertex belongs to a $T + V$ critical line set of codimension $1 + 2 = 3$ (it is a 1D set).

There is also a different kind of multilocal event that was not described in [DDP96]. A segment can be tangent to two objects and belong to one of their common tangent planes. In this case, the common tangent plane adds one codimension and we use the notation $++$. For example $T + +T$ critical

Dimension	Type	Configuration
3	T	
2	T+T	
	V	
1	T+T+T	
	T++T	
	T+V	
0	T+T+T+T	
	T++T+T	
	T+T+V	
	V+V	

Table 1: faces of the visibility complex.

segment sets have codimension $1+1+1 = 3$ (1D set). (One may think of the example of two parallel cylinders and notice that lines contained in a bitangent plane have two degrees of freedom. This case is not considered here because it is degenerated.) These events are crucial for dynamic maintenance of views, aspect graphs and discontinuity meshes. For example a sphere hidden behind another sphere will appear when their outlines are tangent, that is when the viewpoint lies on a $T + +T$ segment.

Each local event corresponds to an algebraic equation: a line tangent to an algebraic object or going through a vertex. A set of critical segments can thus be associated with the connected set of lines verifying the corresponding set of equations.

Events caused by faces are considered as $T + T$ events since they involve two edges. In the same way, segments going through an edge are $V + V$ events. The reason why the case of vertices (which could be seen as two edges events) is distinguished is that they introduce "discontinuities" at the end of edges and require a specific treatment as we shall see in section 5.4.

4   The 3D Visibility Complex

The *3D visibility complex* is the partition of maximal free segments of 3-space into connected components according to the objects they touch. Its faces of dimension 4 are maximal connected components of segments in general position with the two same objects at their extremities.

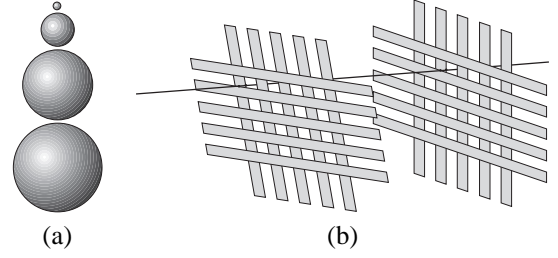The different faces of lower dimension correspond to critical segments as summarized in table 1.

Figure 2: (a) Scene with an $O(n)$ Visibility Complex (b) Scene with an $O(n^4)$ Visibility Complex (an example of $T + T + T + T$ critical line is shown).

Theorem 1 *The size of the 3D visibility complex is $\Omega(n)$ and $O(n^4)$ where n is the complexity of the scene.*

Proof (sketched)

The number of $(k+1)$-faces adjacent to a k-face is bounded. For example a 1-face $T_1+T_2+T_3$ is adjacent to five 2-faces: two faces $T_1 + T_2$ (there are two different faces because one extremity of the segments can lie on the object tangent at T_2 or not. See [DDP96]), $T_1 + T_3$ and two $T_2 + T_3$.

Each 4-face is adjacent to at least one 3-face, a 3-face to at least one 2-face, and a 2-face to at least one 1-face. We just sketch the demonstration. For a given face F of the complex, we consider the associated critical line set S. This set of lines contains a line set S' with one more codimension (one of the lines tangent to one object is also tangent to a second object, one of the lines tangent to two objects belongs to one of their common tangent plane, and one line going through a vertex is tangent to an object). Consider a continuous path from the line associated with a segment s of F to one of S', and the corresponding continuous path over the segments. If all the segments of this path have the same extremities, F is adjacent to the face with one more codimension associated with S, otherwise when the extremity changes there is a tangency local event and one more codimension.

Note that a 1-face may be adjacent to no 0-face (we give an example below of a scene without a 0-face).

So the size of the complex is bounded by the number of 1-faces which are not adjacent to a 0-face plus the number of 0-faces. For each kind of events, the number of possible systems of algebraic equations depends on the number of objects implicated, the $T+T+T+T$ critical line sets are thus the most numerous with $O(n^4)$.

We show in figure 2(a) an example of a scene with a visibility complex of size $O(n)$: there is one $T + +T$ face for each pair of neighbour spheres. Note there is no 0-face in that case. The scene in figure 2(b) is the same as in [PD90] and has an $O(n^4)$ visibility complex. There are two "grids", each one composed of two very slightly distant orthogonal sets of $\frac{n}{4}$ parallel rectangles (this is also valid with thin ellipsoids). Consider a rectangle in each of the four sets: there is always a $T + T + T + T$ critical segment.
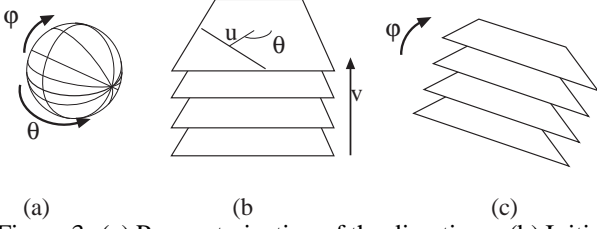
Figure 3: (a) Parameterization of the directions. (b) Initial v sweep (c) φ sweep.

Visual events considered in the aspect graph literature [EBD92, PD90] correspond to the 1-faces of the visibility complex. For example the topology of a view changes when a vertex and an edge are aligned from the viewpoint. The aspect graph is in fact the arrangement of those events in the viewing space. This explains its size: $O(n^6)$ in the orthographic case where the viewing space is S^2 and $O(n^9)$ in the perspective case where the viewing space is R^3.

In [DDP97] we presented a data-structure called the *Visibility Skeleton* which corresponds to the graph of the 0 and 1-faces of the visibility complex. First experiments with a few typical computer-graphics scenes show that the number of these faces (and thus the size of the complex) is about quadratic in the number of input polygons.

5 Output-sensitive sweep

Our algorithm is a double sweep with a preprocessing phase. First the scene is swept by a horizontal plane and a 2D Visibility Complex [PV96] of the φv-slice is maintained (figure 3(b)). We then sweep φ (figure 3(c)), but some 0-faces can not be detected during this sweep and have to be preprocessed.

5.1 Sweeping the initial slice

To build the initial φ-slice, we first maintain a φv-slice of the 3D visibility complex which corresponds to the 2D visibility complex [PV96] of the sweeping plane. We briefly review the 2D visibility complex. It is the partition of the segments of the planes according to the objects they touch. Its 2D faces are connected components of segments touching the same objects (they are φv-slices of the 4-faces of the 3D visibility complex). They are bounded by edges which correspond to segments tangent to one object (φv slices of the 3-faces T) and vertices which are free bitangents of the 2D scene (φv-slices of 2-faces $T + T$). Since a view around a point corresponds to the extremities of the segments going through this point, it corresponds to the traversal of the 2D visibility complex along the 1D path of these segments. The object seen changes when the path traverses a new face, which occurs at an edge of the 2D complex. In the case of a polygon, the chain of edges of the 2D complex going through one of its vertices is the view around this vertex.
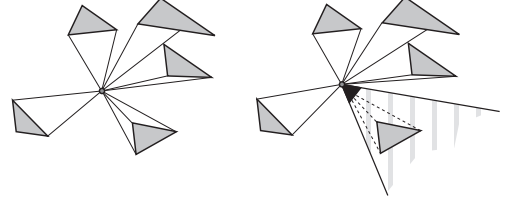

Figure 4: When the first vertex of a polyhedron is swept, the 2D view is computed in the sweeping plane and is restricted for each edge adjacent to the vertex by considering the angle formed by the direction of the two adjacent polygons.
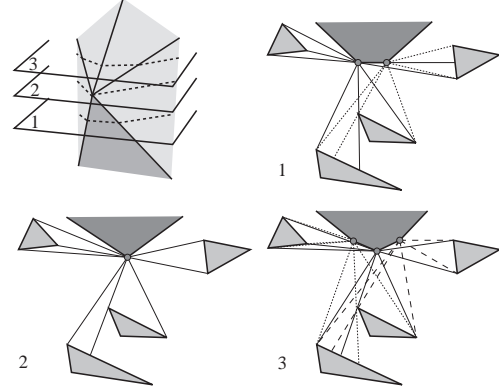

Figure 5: Fusion-restriction of a view around edges when a vertex is swept

The 2D visibility complex has to be updated when the sweeping plane is tangent to an object or contains a vertex and when three 2D slices of objects share a tangent.

When the sweeping plane starts intersecting an object, we have to "insert" this object in our 2D complex. This is done by computing a view around the point of tangency or around the vertex using the current 2D visibility complex. This can be done in $O(v \log n)$ where v is the size of the view using the techniques described in [Riv97]. When the path of this view crosses an edge of the 2D complex it corresponds to a new $T + T$ or $V + T$ face of our 3D complex. In the case of the first vertex of a polygon, the view has to be restricted for each edge of the polyhedron, corresponding to the view seen by a vertex of the 2D slice (see figure 4).

Symmetrically, when an object stops intersecting the sweeping plane, the corresponding faces of the 2D visibility complex are collapsed. These faces are those along the chains of edges corresponding to segments tangent to this object. Their removal can be done in $O(v)$ where v is again the size of the view.

When a vertex in the middle of a polyhedron is encountered the 2D views around the points corresponding to the edges under the vertex have to be merged, and then the view around this vertex has to be restricted for each edge above the vertex, in the same manner as first vertex sweep-events, see figure 5. Each operation is linear in the size of each view.

As the plane moves, three slices of objects can share a tan-

gent (corresponding to a $T+T+T$ face of the 3D complex), in which case the 2D visibility complex is updated using the technique of [Riv97]. Basically, for each bitangent we compute the value of v where it will become tangent to a third object and store these sweep-events in our queue which requires time $O(\log n)$ whenever a bitangent is created.

Finally, a bitangent of the 2D complex can correspond to a common tangent plane. For each bitangent, we compute the value of v for which it will lie on a bitangent plane and insert this sweep-event in the queue. Of course, these sweep-events have to be discarded if the bitangent is collapsed before.

5.2 Principle of the φ sweep

We now have computed a φ-slice of the 3D visibility complex. It is the partition of the segments contained in the set of horizontal planes. In this φ-slice, 1-faces of the complex have dimension 0, 2-faces have dimension 1, and so on.

During the φ-sweep (fig. 8(c)) we maintain this φ-slice as well as a priority queue of sweep-events. In what follows, we will only describe the update of the 1-faces of the visibility complex, the update of the upper dimensional is done at each sweep-event using a catalogue of adjacencies of the 1-faces which for reason of place cannot be given here. As stated before, the number of adjacent upper-dimensional faces is bounded; their update does not affect the complexity.

We first prove that some sweep-events are regular: a 1D component of the φ-slice is collapsed as its two extremities merge. These sweep-events can be detected by computed for each 1D component of the φ-slice the value of φ for which it will collapse. We will then study the case of irregular sweep-events.

5.3 Regular 0-faces

Consider a $T_1 + T_2 + T_3 + T_4$ segments with extremities O_0 and O_5 and elevation angle φ_0 (fig. 6). Consider the $1D$ critical line set $T_1 + T_2 + T_3$. We locally parameterize it by φ and call it $l(\varphi)$. The ruled surface described by $l(\varphi)$ cuts O_4 at φ_0. Two 1-faces of the complex are associated with $l(\varphi)$, one for $\varphi < \varphi_0$ and one for $\varphi > \varphi_0$; one has O_5 at its extremity, the other O_4. It is the same for $T_2 + T_3 + T_4$. Moreover the two 1-faces before φ_0 are adjacent to a 2-face $T_2 + T_3$. In the φ-slice, this 2-face is a 1D set bounded by the slices of $T_1 + T_2 + T_3$ and $T_2 + T_3 + T_4$. This 1D set collapses at φ_0, it is thus a regular sweep-event. It can be detected by considering the adjacent $T + T + T$ faces in the φ-slice and maintaining a priority queue.

The $T + +T + T$ faces can be handled the same way because they are adjacent to a pair of $T + +T$ and a pair of $T + T + T$ 1-faces, and the faces of a pair are associated with the same line set.
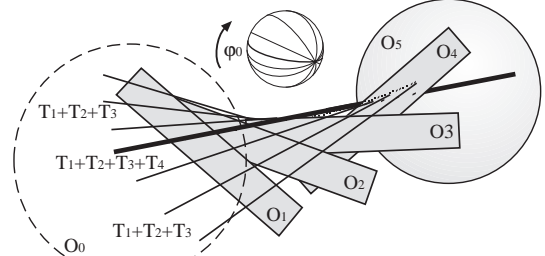

Figure 6: $T + T + T$ critical line set adjacent to a $T + T + T + T$ critical line.
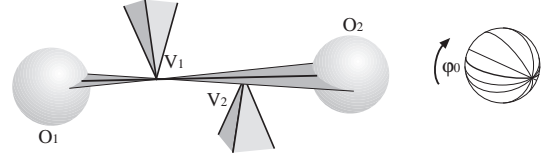

Figure 7: None of the $T + V$ critical segment sets adjacent to this $V + V$ critical segment exist before φ_0

5.4 Irregular 0-faces

Unfortunately, all the 0-faces are not regular sweep-events. The $T + T + V$ and $V + V$ events cannot be detected in this way. The main reason is that vertices represent discontinuities at the end of edges, and we have no guarantee that a 1-face adjacent to such a 0-face exists for $\varphi < \varphi_0$. See figure 7 where the four $T + V$ faces appear at φ_0; this corresponds in the dual space to situation (b) of fig. 8.

These events thus have to be preprocessed by considering all the VV pairs and all the Object-Object-V triplets.

Fortunately, at least one slice of an adjacent 2-face exists before such 0-faces appear (face V_1 in fig 7). The proof is omitted from this version. This face is found using a search structure over the 1D components of the φ-slice ordered by their generators. The 0-face is then tested for occlusion: we test if the generators (V_2 here) lies between the extremities (O_1 and O_2) of the 2-face. It can then be inserted.

5.5 Non monotonic 1-faces

There is another kind of irregular sweep-event. A 1-face of the complex can appear during the sweep without a 0-face event. This is obviously the case for $T + +T$ events since they can be adjacent to no 0-face, but this can also be the case for $T + T + T$ events. Consider the associated line set, it is not necessarily monotonic with respect to φ (see fig. 8(c)). These sweep-events also have to be preprocessed and inserted in the φ-slice with a search over the 1D components.

5.6 Complexity of the algorithm

Theorem 2 *The visibility complex can be built in time $O((k + n^3) \log n)$ where n is the complexity of the scene, and k the number of 0-faces of the complex.*
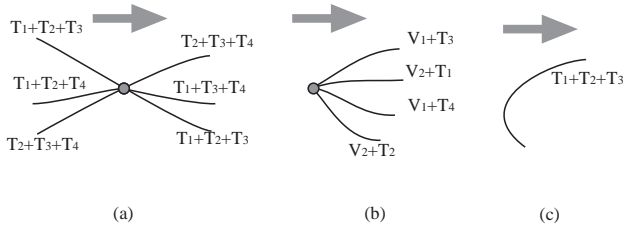
Figure 8: Different sweep-events represented in the dual space. The $T+T+T+T$ event (a) is regular, but the $V+V$ event (b) has to be preprocessed as well as the null derivative with respect to φ of the $T+T+T$ events (c).

During the initial v sweep, each view computation requires time $O(v \log n)$ where v is the size of the view. A view corresponds to the number of 3-faces of the 3d visibility complex adjacent to the appearing/disappearing 2 faces. The total cost is thus bounded by $O(k \log n)$. Each tritangent event requires time $O(\log n)$, here again the cost is bounded by $O(k \log n)$.

During the φ sweep, each regular event requires $O(\log n)$ to maintain the priority queue.

The preprocessing of the other 0-faces and non-monotonic 1-faces requires the enumeration of all the triplets of objects and the insertion of the computed faces in the priority queue, it is therefore $O(n^3 \log n)$.

The output-sensitive nature of this algorithm is very important since experiments on a few polygonal scenes [DDP97] have shown that the number of $T+T+T+T$ segments which is responsible of the theoretical $O(n^4)$ is in fact much less than the number of $T+T+V$ segments.

6 Conclusions and future work

We have introduced a unified data structure, the 3D visibility complex, which encodes the global visibility informations for 3D scenes of polygons and convex smooth objects. Its size k is $\Omega(n)$ and $O(n^4)$ and we have presented an output-sensitive algorithm to build the structure in time $O((n^3 + k) \log n)$.

Future work includes the use of the visibility complex to maintain views around a moving viewpoint, a study of the events involved by concave and piecewise smooth objects, the development of a better construction algorithm, and the incremental update of the visibility complex when an object is moved, added or removed.

Acknowledgments

References

[CEG+96] B. Chazelle, H. Edelsbrunner, L. J. Guibas, M. Sharir, and J. Stolfi. Lines in space: combinatorics and algorithms. *Algorithmica*, 15:428–447, 1996.

[DDP96] F. Durand, G. Drettakis, and C. Puech. The 3d visibility complex, a new approach to the problems of accurate visibility. In *Proc. of 7th Eurographics Workshop on Rendering in Porto, Portugal*, June 1996.

[DDP97] F. Durand, G. Drettakis, and C. Puech. The visibility skeleton: A powerful and efficient multi-purpose global visibility tool. *Computer Graphics (Siggraph'97 Proceedings)*, 1997.

[DF94] G. Drettakis and E. Fiume. A fast shadow algorithm for area light sources using back projection. In *Computer Graphics Proceedings, Annual Conference Series:* SIGGRAPH '94 (Orlando, FL), July 1994.

[EBD92] D. Eggert, K. Bowyer, and C. Dyer. Aspect graphs: State-of-the-art and applications in digital photogrammetry. In *Proceedings of the 17th Congress of the Int. Society for Photogrammetry and Remote Sensing*, 1992.

[LTG93] D. Lischinski, F. Tampieri, and D. Greenberg. Combining hierarchical radiosity and discontinuity meshing. In *Computer Graphics Proceedings, Annual Conference Series:* SIGGRAPH '93 (Anaheim, CA, USA), August 1993.

[MS97] S. Mohaban and M. Sharir. Ray shooting amidst spheres in 3 dimensions and related problems. *to appear in SIAM J. Computing*, 1997.

[ORDP96] R. Orti, S. Rivière, F. Durand, and C. Puech. Radiosity for dynamic scenes in flatland with the visibility complex. In *Proc. of Eurographics*, Poitiers, France, 1996.

[PD90] H. Plantinga and C. R. Dyer. Visibility, occlusion, and the aspect graph. *IJCV*, 1990.

[PDS90] H. Plantinga, C. R. Dyer, and B. Seales. Real-time hidden-line elimination for a rotating polyhedral scene using the aspect representation. In *Proceedings of Graphics Interface '90*, 1990.

[Pel90] M. Pellegrini. Stabbing and ray shooting in 3-dimensional space. In *Proc. 6th Annu. ACM Sympos. Comput. Geom.*, 1990.

[PPK92] S. Petitjean, J. Ponce, and D.J. Kriegman. Computing exact aspect graphs of curved objects: Algebraic surfaces. *IJCV*, 1992.

[PV96] M. Pocchiola and G. Vegter. Topologically sweeping visibility complexes via pseudo-triangulations. *Discrete Comput. Geom.*, December 1996. special issue devoted to ACM-SoCG'95.

[PV96] M. Pocchiola and G. Vegter. The visibility complex. *Internat. J. Comput. Geom. Appl.*, 96. special issue devoted to ACM-SoCG'93.

[Rie87] J.H. Rieger. On the classification of views of piecewise smooth objects. *Image and Vision Computing*, 1987.

[Riv97] S. Rivière. Dynamic visibility in polygonal scenes with the visibility complex. In *Proc. 13th Annu. ACM Sympos. Computat. Geom.*, 1997.

[SG94] J. Stewart and S. Ghali. Fast computation of shadow boundaries using spatial coherence and backprojections. In *Proceedings of SIGGRAPH '94 (Orlando, Florida, July 1994)*, Computer Graphics Proceedings, July 1994.

[Tel92] S. Teller. Computing the antipenumbra of an area light source. *Computer Graphics*, July 1992. Proceedings of SIGGRAPH '92 in Chicago (USA).